Phase-sensitive tests of the symmetry of the pairing state in the high-temperature superconductors—Evidence for $d_{x^2-y^2}$ symmetry

D. J. Van Harlingen

Department of Physics and Materials Research Laboratory, University of Illinois at Urbana-Champaign, Urbana, Illinois 61801

Understanding the mechanism responsible for superconductivity in the high-temperature cuprates has been one of the major goals of condensed-matter physicists since the discovery of these exciting materials in 1986. Experimental evidence suggests that the pairing state may be unconventional, featuring an anisotropic order parameter for which a wide range of theoretical models for the superconducting pairing have been proposed. Recently, a new class of experiments has been presented that are sensitive to the phase of the superconducting order parameter, allowing an unambiguous determination of the symmetry of the pairing state. These experiments, based on the interference of the quantum-mechanical phases in Josephson tunnel junctions and dc SQUID devices, give strong evidence for pairing in a channel with d-wave symmetry in the most widely studied cuprate, $YBa_2Cu_3O_{7-x}$. Confirmation of this pairing state will focus efforts to develop a microscopic theory for the high-temperature superconductors and to apply them in power transmission and electronic device technologies.

CONTENTS

I. INTRODUCTION

One of the most capitivating ongoing debates in condensed-matter physics is the question of the symmetry of the pairing state and its underlying mechanism in the high-temperature superconductors. Since their discovery in 1986, a growing list of theoretical calculations and experiments have suggested that the high-temperature cuprates may exhibit an unconventional pairing state. By unconventional, we mean a state with an order parameter or energy gap that has a symmetry in momentum space different from that of the isotropic s-wave Cooper pair state that is believed to describe almost all low-temperature superconductors. Much of the recent attention has been focused on a particular state with d-wave symmetry, the $d_{x^2-y^2}$ pairing state. This state has two key properties that make it a feasible candidate for explaining the behavior of the cuprates. First, it exhibits nodes in the energy gap that lead to an excess of excitations at low temperatures. The presence of such excitations has been firmly established by a host of transport, tunneling, and thermodynamic measurements over the past eight years. Second, this particular d-wave symmetry is implied by a number of possible superconducting pairing mechanisms, particularly those involving magnetic interactions that are known to be important in the cuprates. However many other pairing symmetries are also possible and have been promoted in the framework of theoretical models and experimental results. The determination of the order-parameter symmetry is a crucial first step in identifying the pairing mechanism and in the subsequent development of a microscopic theory for high-temperature superconductivity. It may also be important in the application of the high-temperature superconductor materials for electronic device and power transmission technologies.

The challenge for experimentalists is to derive tests that are capable of distinguishing the candidate pairing states and to make an unambiguous determination of the pairing-state symmetry. This turns out to be a rather formidable task. Most experiments measure the *magnitude* of the order parameter and exhibit only a subtle dependence on the symmetry of the pairing state. Further, the intrinsic complexity of the cuprates and the paucity of

 0034-6861/95/67(2)/515(22)/$10.30

high-quality samples has led to contradictory results and confusion in the interpretation of experimental data relevant to the pairing symmetry. For these reasons, it is impossible to make a convincing determination of the pairing symmetry from magnitude measurements alone.

In this Colloquium, we discuss a new class of experiments designed to determine the pairing-state symmetry by looking at the phase coherence of tunnel junctions and SQUID devices incorporating the high-temperature superconductors. The key feature of these experiments is their sensitivity to the anisotropy of the *phase* of the order parameter rather than to its magnitude. This enables a direct test of the most unique and characteristic feature of the proposed d-wave state—the sign change in the order parameter in different k-space directions. Since these experiments probe the phase directly, they give clear and striking indications of the symmetry and are largely impervious to the effects of impurities and sample quality. From our original experiments and subsequent variations of them a clear and consistent picture is emerging: there now seems to be nearly incontrovertible evidence for a pairing state with at least a large component of d-wave symmetry in the cuprate $YBa_2Cu_3O_{7-x}$. If so, this would be the first confirmed example of an unconventional pairing state in superconductivity and would open up important and exciting channels for experimental and theoretical research on the details and implications of such an exotic system.

My plan in this paper is the following. I first outline the most feasible candidate states and how one might go about distinguishing them experimentally. Next, I discuss the fundamental basis for the phase-sensitive determination of the symmetry. I then describe in detail the design, implementation, and results of the two specific experiments we have conducted at the University of Illinois that have for the first time given strong direct experimental evidence for a pairing state with $d_{x^2-y^2}$ symmetry. Finally, I briefly review additional experiments that are also sensitive to the phase of the order parameter and that for the most part, but not in every case, confirm the evidence for d-wave symmetry that we find in our experiments.

II. BACKGROUND

A. Conventional superconductors

The superconductivity in most materials is known to result from a pairing of electrons via an attractive phonon-mediated electron-electron interaction that can dominate the usual Coulomb repulsion at low temperatures, as illustrated in Fig. 1(a) (Bardeen *et al.*, 1957). The ground state is a spin-singlet state in which electrons of opposite spin and momentum are effectively paired. These Cooper pairs form a condensate that can be described by a single quantum-mechanical phase, leading to long-range macroscopic phase coherence that is one of

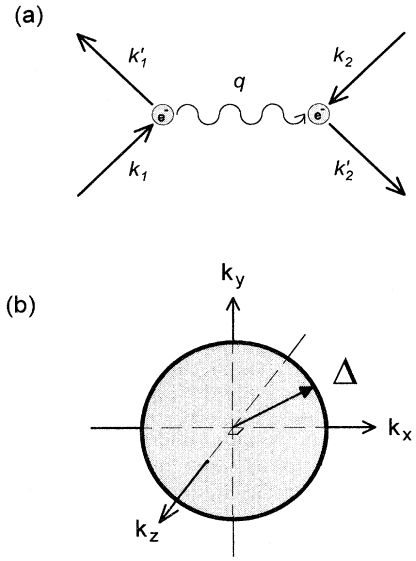

FIG. 1. The conventional picture of superconductivity: (a) In the BCS model, superconductivity arises from the attractive electron-electron interaction mediated by phonon scattering. (b) The excitations from the Cooper pair ground state exhibit an energy gap Δ that is (very nearly) isotropic in k space.

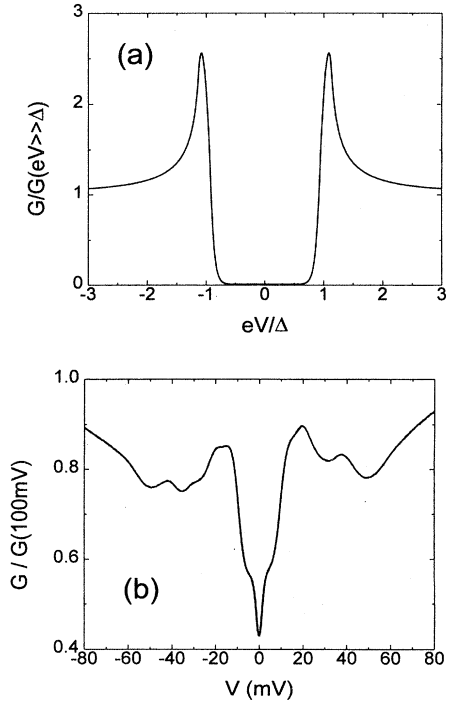

FIG. 2. Tunneling characteristics are the most sensitive probe of the energy-gap structure of superconductors: (a) Single-particle tunneling conductance vs voltage for tunneling from a normal metal into an isotropic s-wave superconductor, showing the absence of states below the threshold for conductance at voltage Δ/e. (b) Conductance measured for a YBCO-Pb tunnel junction, showing excess states below the energy gap expected from the BCS theory. This is typical of tunneling curves observed in the cuprates, which never exhibit a fully formed gap.

the unique signatures of the superconducting state. The excitations from the ground state involve mixtures of electron and hole states referred to as quasiparticles. One of the most striking properties of the quasiparticles is that they exhibit an energy gap $\Delta(\mathbf{k})$ with respect to the ground-state energy. In conventional superconductors, the energy gap is very nearly isotropic in k space, so that the gap has the same magnitude and phase in all directions, as shown in Fig. 1(b). We refer to this as an isotropic s-wave pairing state.

The energy gap inhibits the creation of excitations in the superconducting state and dominates the low-temperature electrical transport and optical properties of superconductors. The energy gap is most clearly demonstrated and measured by tunneling measurements into superconductors that exhibit a sharp conductance increase at voltage $V=\Delta/e$, as in Fig. 2(a) (Giaver, 1960). With the exception of a class of materials referred to as the heavy-fermion superconductors, all low-temperature superconducting materials are believed to result from the BCS phonon-coupling mechanism and exhibit this pairing symmetry.

B. High-temperature cuprate superconductors

The high-temperature cuprates are highly anisotropic layered materials in which the superconductivity is believed to occur in two-dimensional CuO_2 planes that are weakly coupled to each other via Josephson tunneling (Josephson, 1962). Following their discovery (Bednorz and Müller, 1986), it was quickly recognized that these materials did not behave as ordinary BCS superconductors. In the first place, the transition temperatures of the cuprates (>80 K) appeared too high to be explained by a phonon-coupling mechanism. Further, although there is substantial evidence for electron pairing, there are also extensive experimental data that show that the energy gap is not fully formed. This shows up prominently in tunneling measurements that display a high sub-gap density of states, as in Fig. 2(b), and indirectly in thermodynamic, transport, and optical properties that exhibit power-law rather than exponential temperature dependences at low temperature. In addition, the cuprates exhibit strong magnetic interactions in the form of antiferromagnetic spin correlations that are usually mutually exclusive with superconductivity. These considerations have motivated the investigation of almost every conceivable mechanism that could create a pairing interaction sufficiently strong to yield superconductivity at these elevated temperatures; strongly correlated models that have been proposed to explain the cuprates have been recently reviewed by Dagotto (1994). The most distinguishing feature of each proposed model is its prediction for the symmetry of the order parameter implied by the specific pairing mechanism.

III. CANDIDATE PAIRING STATES

There are many allowed symmetries for the pairing state of superconductors; the full range has been catalogued by Annett, Goldenfeld, and Renn (1991), who also made a comprehensive review of the experimental evidence for different symmetries up to that time. The temperature dependence of the NMR relaxation rates is generally viewed as providing direct evidence of spin-singlet pairing (Barrett *et al.*, 1991), restricting the candidates to states with s-wave or d-wave symmetry. There are also indications that spin fluctuations, thought to be important in the normal state, may also be responsible for the superconductivity. It was first suggested within the framework of a Hubbard model by Scalapino and co-workers (Bickers *et al.*, 1989) that the exchange of antiferromagnetic spin fluctuations could promote pairing in a $d_{x^2-y^2}$ channel, but this mechanism was at the time believed to be too weak to explain the high transition temperatures of the cuprates. However, detailed calculations by Pines and co-workers within a phenomenological model (Monthoux, Balatsky, and Pines, 1992; Monthoux and Pines, 1993, 1994) and independently by Moriya and co-workers by a self-consistent renormalization approach (Moriya *et al.*, 1990; Ueda, 1992) showed that a complete treatment of the coupling of quasiparticles by magnetic interactions inevitably leads to $d_{x^2-y^2}$ symmetry and provides sufficient coupling to account for the observed transition temperatures. The motivation for this model and the parameters incorporated in it are largely derived from NMR measurements (for a review, see Slichter, 1994). The spin-fluctuation model predicts many of the normal and superconducting-state properties of the cuprates, and is supported by many recent experiments (see the recent review by Pines, 1995). From an experimental viewpoint, the prediction of the $d_{x^2-y^2}$ symmetry was a significant step, since it put on the table a testable hypothesis that has motivated a tremendous wave of experiments designed to determine the pairing symmetry.

The energy gap (order parameter) of the $d_{x^2-y^2}$ state has the functional form in k space

$$[d_{x^2-y^2}]\quad \Delta(\mathbf{k})=\Delta_0[\cos(k_x a)-\cos(k_y a)]\ , \tag{1}$$

where Δ_0 is the maximum gap value and a is the in-plane lattice constant. The gap is real with a strongly anisotropic magnitude featuring nodes along the (110) directions in k space and a sign change in the order parameter between the lobes in the k_x and k_y directions. Physically, this sign change indicates a relative phase of π in the superconducting condensate wave function for Cooper pairs with orthogonal relative momenta. In the cuprates, this state is believed to describe the order parameter in the CuO_2 planes, with the lobes being aligned with the in-plane lattice vectors.

Alternate theoretical models invoking conventional phonon coupling enhanced by tunneling between adjacent CuO_2 planes in the cuprate structure argue for an anisotropic s-wave symmetry. In this state, the order parameter has a single sign but is partially suppressed in magnitude along the (110) lines. One form of this state that was suggested by Anderson, Chakravarty, and coworkers (Chakravarty *et al.*, 1993) has the form

$$[\text{anisotropic } s] \quad \Delta(\mathbf{k})=\Delta_0[\cos(k_x a)-\cos(k_y a)]^4+\Delta_1 \ . \tag{2}$$

Here, Δ_1 represents the minimum value of the gap, which occurs along the (110) directions. It has also been suggested that very strong anisotropic suppression of the order-parameter magnitude along the (110) directions could result in a sign change in the order parameter for a range of angles along those directions. This state has been referred to as the extended s-wave state (Brandow, 1994; Scalapino, 1995), but in symmetry terms is actually an $s+g$ state. A possible functional form of this state is

$$[\text{extended } s \text{ wave}] \quad \Delta(\mathbf{k})=\Delta_0\{(1+\gamma^2)[\cos(k_x a)-\cos(k_y a)]^2-\gamma^2\} \ , \tag{3}$$

which features eight lobes of alternating signs and eight nodes split by approximately $\pm\gamma\pi/2$ from the (110) directions.

Complex mixture states such as the $s+id$ states (Kotliar, 1988; Li *et al.*, 1993) and the anyon state $d_{x^2-y^2}+id_{xy}$ (Rokhsar, 1993; Laughlin, 1995) are also allowed by symmetry and have been proposed. These have the form

$$[s+id] \quad \Delta(\mathbf{k})=\Delta_0\{\varepsilon+i(1-\varepsilon)[\cos(k_x a)-\cos(k_y a)]\} \ , \tag{4}$$

$$[d+id] \quad \Delta(\mathbf{k})=\Delta_0\{(1-\varepsilon)[\cos(k_x a)-\cos(k_y a)]+i\varepsilon[2\sin(k_x a)\sin(k_y a)]\} \ . \tag{5}$$

In each case, ε is the fraction of s or d_{xy} component mixed in with the $d_{x^2-y^2}$ state, and $\varepsilon\Delta_0$ is the minimum energy gap. These complex mixture states are of particular interest because the order parameter is complex and breaks time-reversal symmetry. However, at present there is no experimental indication of this phenomenon in the cuprates. As a result, the two leading candidates for the pairing symmetry are the pure $d_{x^2-y^2}$ and the anisotropic s-wave state.

IV. DETERMINING THE SYMMETRY BY EXPERIMENT

Experimental determination of the symmetry of the pairing state requires a direct measurement of the anisotropy of the order parameter. Strategies for distinguishing between the proposed symmetries are best seen by plotting the *magnitude* and the *phase* of the order parameter as a function of k-space direction for the primary candidate states, as in Fig. 3.

A. Magnitude measurements

Most experiments are sensitive only to the magnitude of the order parameter. For symmetries other than the conventional isotropic s wave, the magnitude exhibits a modulation with fourfold rotation symmetry. In the $d_{x^2-y^2}$ state, there are true nodes along the (110) directions. Nodes also exist in the extended s-wave state, but they are split and shifted from the diagonal directions. In contrast, the anisotropic s-wave state exhibits only a depression along the (110) direction, with a depth that depends on the details of the model. For the mixture states, the minimum gap depends on the mixture fraction of the s- and d-wave states. In all of the anisotropic cases, the reduced gap in some directions leads to an excess number of excited quasiparticles, which shows up strongly in low-temperature transport and tunneling spectra. The increased excitation density over that expected for a fully gapped superconductor has been documented by countless experiments since the discovery of the cuprates and is now generally accepted to be an intrinsic property of these materials. Several experiments, including angle-resolved photoemission (Shen *et al.*, 1993), NMR spectroscopy (Martindale *et al.*, 1993), Raman scattering (Devereaux *et al.*, 1994), scanning tunneling microscopy (Kane *et al.*, 1994), and thermal conductivity in a magnetic field (Yu *et al.*, 1995) have even probed the spatial anisotropy directly, finding evidence for a fourfold modulated magnitude in which the order parameter drops to no more than 20% of its maximum value along the diagonal directions. So far, the most sensitive magnitude probe is the measurement of the low-temperature penetration depth. Early penetration depth experiments in YBCO were interpreted as being exponential at low temperatures and cited as evidence for conventional s-wave pairing, but a careful reanalysis of the data (Annett *et al.*, 1991) showed that the data were better described by a power law, indicative of an anisotropic gap. Using a precision microwave resonator technique and high-quality single crystals of YBCO, Hardy, Bonn, and co-workers at UBC found that the penetration depth is linear down to about 2 K, implying line nodes that are at most 2% of the full gap value (Hardy *et al.*, 1993; Hirschfeld and Goldenfeld, 1993). Impurity doping into these crystals produces a quadratic term, explaining why this dependence, rather than the linear contribution, is usually seen in YBCO crystals and always dominates in thin films (Bonn *et al.*, 1995). Thus the anisotropy of the gap magnitude is well established by experiment and seems to be significant. Nonetheless, because impurities

can either obscure or mimic the presence of true nodes, it is not possible to determine the symmetry of the pairing state unambiguously from magnitude measurements alone.

B. Phase measurements

An alternative approach is to probe the relative phase of the order parameter as a function of k-space direction.

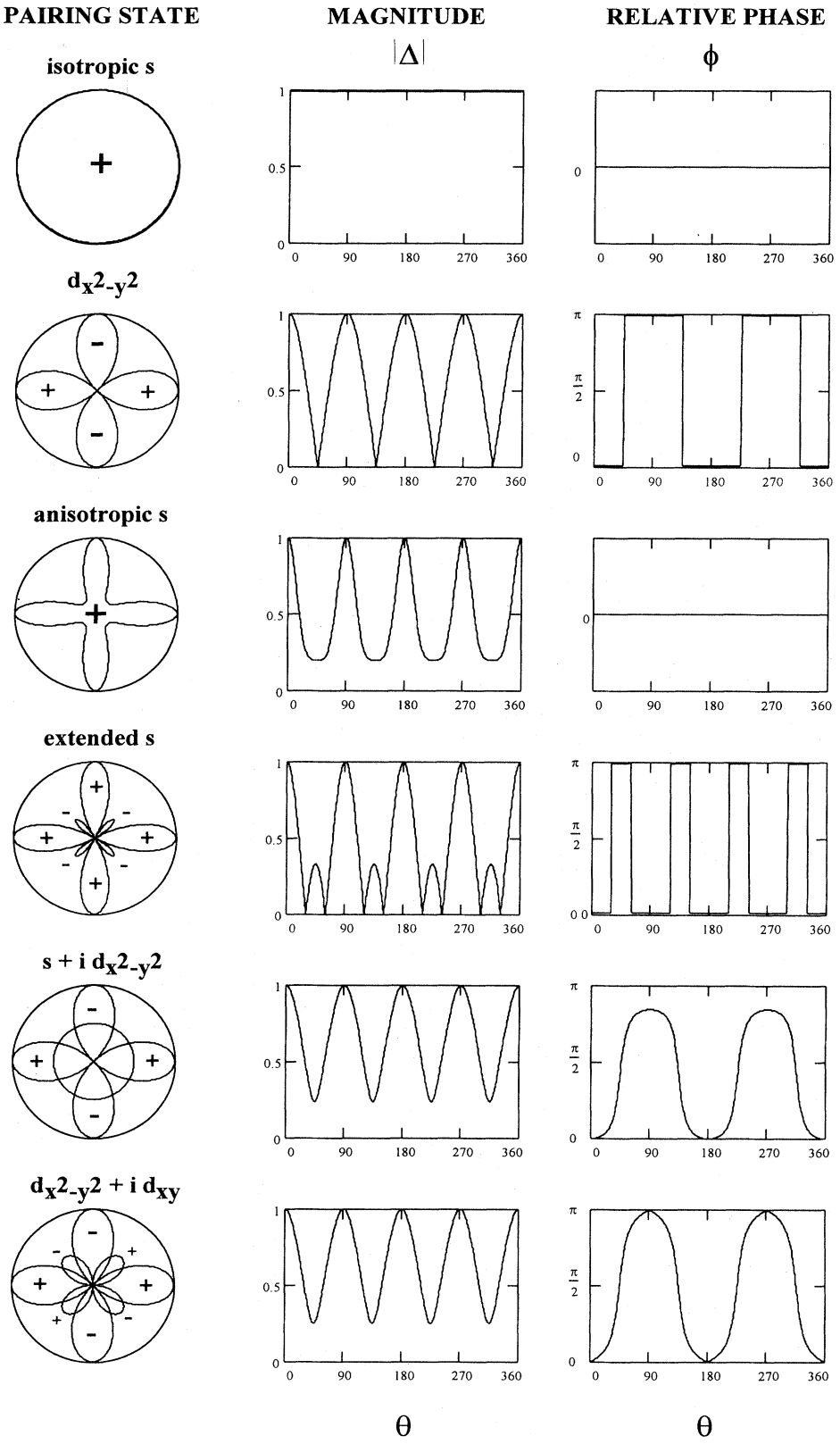

FIG. 3. Magnitude and phase of the superconducting order parameter as a function of direction in the CuO_2 planes of the cuprates for the primary candidates for the pairing symmetry. This suggests possible approaches to experimentally determining the symmetry.

The phase is distinctly different for the various candidate states. In particular, the *s*-wave states (isotropic or anisotropic) and the *d*-wave states are clearly distinguished, since the *s*-wave state has a uniform phase whereas the *d*-wave state exhibits discontinuous jumps of π at the (110) lines, reflecting the sign change in the order parameter in orthogonal directions. In the extended *s*-wave state, there are also π-phase jumps but overall invariance under 90° rotation. For the $s+id$ and $d+id$ mixture states, the phase varies continuously with angle.

To exploit these differences, it is necessary to devise an experiment that is capable of sensing the phase of the order parameter in particular directions and measuring its relative phase. The most direct way to accomplish this is to carry out an interferometer experiment comparing the phases in orthogonal directions. We have proposed two related schemes for carrying out the interferometry measurements: our original approach based on a dc SQUID, and an alternate approach based on single Josephson junctions. These are analogous, respectively, to two-slit interference and single-slit diffraction measurements traditionally used to extract relative phases in optical systems.

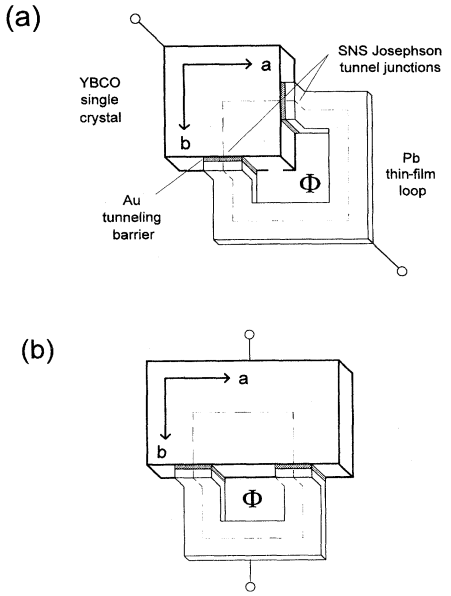

FIG. 4. Design of the SQUID experiments: (a) Configuration of the corner SQUID interferometer experiment used to determine the relative phase between orthogonal directions. (b) Configuration of the edge SQUIDs used as a control sample, in which both junctions are on the same crystal face.

V. DC SQUID EXPERIMENTS

Our basic scheme for measuring the relative phase anisotropy of the superconducting order parameter is shown in Fig. 4(a). We form Josephson tunnel junctions on the orthogonal faces of a single crystal of a high-temperature superconductor. The junctions are joined by a loop of a conventional *s*-wave superconductor, forming a bimetallic ring. This circuit is a two-junction interferometer or dc SQUID (superconducting quantum interference device), a configuration that has been extensively studied. The electronic properties of this device are a periodic function of the magnetic flux applied to the loop and, as we shall discuss, depend in a dramatic way on the intrinsic phase drop inside the crystal. The basic idea for this scheme was suggested to us by A. J. Leggett, but actually first appeared in the literature in a paper by Geshkenbein, Larkin, and Barone (1987) as a test for possible axial *p*-wave symmetry in the heavy-fermion superconductors. It was also independently arrived at by Sigrist and Rice (1992), who considered *d*-wave pairing as a possible explanation for spontaneous magnetization effects observed in cuprate composites.

A. Concepts

There are two primary keys to this experiment. First, the Josephson tunnel junctions serve as directional probes of the phase of the order parameter inside the crystal. The supercurrent in a Josephson junction depends on the phase difference ϕ between the two superconductors according to $I=I_c\sin\phi$, where I_c is the critical current, the maximum supercurrent that can flow before a voltage develops across the junction. Further, the tunneling is highly directional, so that each junction senses the order parameter in the direction perpendicular to the crystal face. This occurs because the tunneling probability depends strongly on the barrier thickness and hence is highly peaked for forward tunneling. This result is well known for standard oxide-barrier SIS (superconductor-insulator-superconductor) tunnel junctions and has been used to probe gap anisotropies in conventional superconductors (which are at most only a few %). Although not as widely recognized, the directionality of the pair tunneling applies equally to other Josephson weak links, such as the SNS (superconductor-normal metal-superconductor) junctions used in our experiments that support diffusive transport for single-particle excitations (Leggett, 1993). The second key element of the experiment is that the two superconductors and two junctions form a multiply connected loop around which phase coherence of the superconducting order parameter must be maintained in order that the superconducting condensate wave function be single valued. This phase constraint leads to a periodic dependence of the SQUID electronic properties on the applied magnetic field and a sensitivity to intrinsic phase shifts within the superconducting materials arising from the symmetry of the pairing interactions.

We consider a dc SQUID, as in Fig. 4(a), with junction critical currents I_{ca} and I_{cb}. A bias current I applied to the SQUID in the supercurrent state divides through the two junctions

$$I=I_{ca}\sin\phi_a+I_{cb}\sin\phi_b \tag{6}$$

subject to the phase constraint

$$\phi_a - \phi_b + 2\pi \left[\frac{\Phi}{\Phi_0} \right] + \delta_{ab} = 0 \tag{7}$$

on ϕ_a and ϕ_b, the gauge-invariant phase differences across the junctions on the a and b faces of the crystal. Here,

$$\Phi = \Phi_{\text{ext}} + LJ \tag{8}$$

is the magnetic flux in the loop, which includes contributions from externally applied flux Φ_{ext} and flux from the circulating current J around the SQUID loop, which has self-inductance L. The extra term δ_{ab} in Eq. (7) accounts for the intrinsic phase shift inside the YBCO crystal between pairs tunneling into the crystal in the a and b directions. This is the key factor, with $\delta_{ab}=0$ for all of the s-wave states and the $d+id$ state, $\delta_{ab}=\pi$ for $d_{x^2-y^2}$ symmetry, and $\delta_{ab}=(1-\varepsilon)\,\pi$ for an $s+id$ mixture with a fraction ε of s-wave component. For a symmetric dc SQUID with equal junction critical currents $I_{ca}=I_{cb}=I_0$, in the limit of zero loop inductance, the maximum supercurrent modulates with applied flux from a maximum of $2I_0$ all the way down to zero supercurrent, according to

$$I_c(\Phi_{\text{ext}}) = 2I_0 \left| \cos \left[\pi \frac{\Phi_{\text{ext}}}{\Phi_0} + \delta_{ab} \right] \right| . \tag{9}$$

For finite values of the screening parameter $\beta = 2LI_0/\Phi_0$, the modulation depth of the critical current is reduced because the circulating currents generate a flux contribution in the loop. For large β, $\Delta I_c/I_c \sim 1/\beta$.

The two principal cases are indicated in Fig. 5. If the YBCO has s-wave symmetry (isotropic, anisotropic, or extended), the phase of the order parameter is the same at each junction inside the YBCO, so that $\delta_{ab}=0$ and the circuit will behave as an ordinary dc SQUID. In particular, the critical current is a *maximum* for zero applied field, and the circulating current at this point is zero. This behavior will also be exhibited by edge SQUIDs, with the geometry shown in Fig. 4(b), in which both junctions are on the same crystal face, independent of the pairing symmetry, since each junction samples the phase in the same k-space direction. In contrast, for $d_{x^2-y^2}$ symmetry the order parameter has an intrinsic phase shift $\delta_{ab}=\pi$ between the a and b directions in the corner SQUID. At zero flux, the junction currents are exactly out of phase and, for sufficient SQUID inductance, a circulating current must flow to maintain phase coherence around the SQUID loop. As a result, the critical current will instead be a *minimum* at zero flux. If the pairing state has $s+id$ symmetry, the phase shift is $\varepsilon\pi$ and depends on the mixture fraction; for an equal admixture of the s and d components, $\delta_{ab}=\pi/2$. Thus, by observing the modulation of the SQUID response vs applied magnetic flux, it is possible to deduce the symmetry of the pairing state of the YBCO sample. The elegance of the experiment is that it depends only on the relative phases of the order parameter and is not sensitive to the type, size, or critical currents of the constituent junctions.

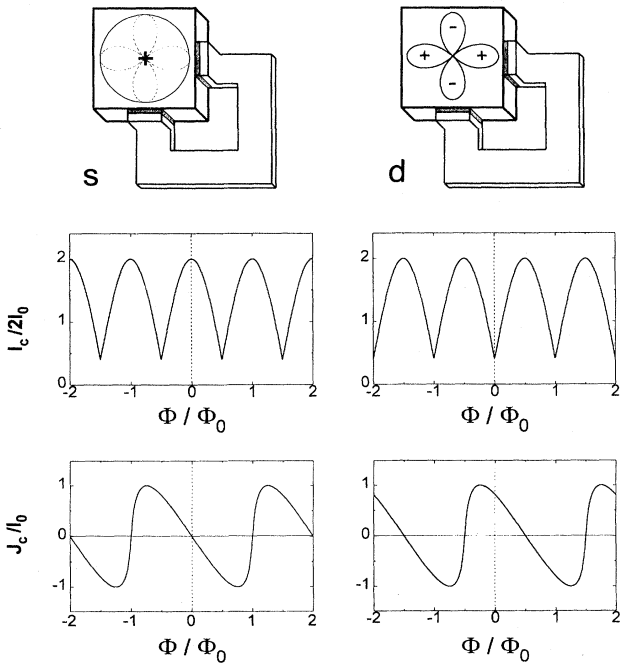

FIG. 5. Modulation of the critical current and circulating supercurrent vs applied magnetic flux for corner SQUIDs with s-wave and d-wave symmetry. The key distinguishing feature is the phase of the modulation curves, characterized by the values of the currents at zero applied field.

B. Complicating issues

Before presenting the details of our experiments and their results, we address several important issues that could impact the results and interpretation of the experimental data: the role of twin boundaries, the related effect of the orthorhombicity of the crystal structure, and complications due to SQUID symmetries, residual magnetic fields, and trapped magnetic flux. These are all factors that we were concerned about prior to carrying out our initial measurements and must be considered in making an unambiguous determination of the pairing symmetry from the SQUID measurements.

1. Twinning

Since YBCO has an orthorhombic crystal structure, it has a tendency to form twin boundaries at which the a and b lattice constants are interchanged. One might think that it would therefore be essential to carry out the SQUID experiments on untwinned single crystals to ensure that the order parameter maintains a single domain throughout the crystal. However, there are both experimental support and theoretical arguments that indicate that the superconducting order parameter maintains its

orientation across twin boundaries and forms a single domain even in twinned samples. The experimental evidence is that we see little difference between the critical currents of junctions prepared the same way on twinned vs untwinned edges. If the order parameter were rotating its orientation at twin boundaries, we would expect the critical current to be reduced by averaging over the twin regions of opposite polarity. We also observe the same results for the phase measurements in twinned and untwinned single crystals, further evidence that the order parameter has a single domain. This result is expected theoretically because the energy cost to rotate the order-parameter polarity at a twin boundary is exceedingly high in our samples. The domain-wall energy is of the order of the Josephson coupling energy across the boundary, $E_J \approx \hbar I_b/2e$, where I_b is the twin-boundary critical current. This factor is large because both the critical current densities of the twin-boundaries and the twin surface areas are very large. In fact, as long as the critical currents of the Josephson junctions on the face (I_c) are small compared to the twin-boundary critical current (I_b), the crystal should maintain a single order-parameter domain. In our single-crystal samples, $I_c \sim 10\ \mu\text{A}-1$ mA and $I_b \sim 10$ A so that this constraint is easily satisfied. The order parameter should also retain its uniformity in highly aligned thin films despite a high density of twins, making it feasible to perform the SQUID experiments described in thin-film samples. A single domain may not, however, be established in thin films with large-angle grain boundaries or in crystals with structural defects for which I_b is substantially smaller.

2. Orthorhombicity

Another consequence of the orthorhombicity of YBCO is that it is likely that a d-wave state in this material would exhibit order-parameter lobes of different sizes, i.e., the + lobes might be larger than the − lobes. This should not directly affect the phase coherence experiments described here, since they are sensitive only to the relative phase, but this could play a role in order-parameter tests that depend on the magnitude. In heavily twinned samples such as thin films, the order parameter will be effectively tetragonal in symmetry, since the order-parameter domains average over many twin domains.

3. SQUID asymmetry

The modulation curves in Fig. 5 pertain to a symmetric SQUID with identical junctions and equal loop arms. Asymmetries between the critical current in the junctions and in the loop inductance can modify the SQUID critical current modulation patterns significantly. In general, the effects of asymmetry are to suppress, skew, and shift the flux modulation pattern. Of particular importance here is a shift in the pattern, since this could mimic or obscure phase shifts arising from the order-parameter symmetry. Most important is the asymmetry in the critical current, characterized by the asymmetry parameter α. If we assume the two junctions have critical currents $I_{ca}=(1-\alpha)I_0$ and $I_{cb}=(1+\alpha)I_0$, the depth of the critical current modulation is reduced from the symmetric case by a factor of $(1-\alpha)$ in the zero-inductance limit. More importantly, in a SQUID with finite inductance, the imbalance in the currents through the two junction arms couples a net magnetic flux to the SQUID loop, shifting the modulation pattern. When the critical current is at its peak, this flux contribution has magnitude $\Delta\Phi=\frac{1}{2}\alpha\beta\Phi_0$, which can be substantial if the inductance and/or asymmetry are large. An additional shift occurs if the inductance of the arms of the SQUID is asymmetric. In these cases, it is necessary to determine the critical current modulation numerically, and extensive calculations have been carried out on SQUIDs of varying geometries. In our experiments, we have been able to make SQUIDs in which the asymmetry is small enough not to be a significant problem, and, for samples in which the asymmetry is significant, have devised a scheme that accounts for asymmetry effects by extracting the intrinsic phase shift in the crystal.

4. Residual magnetic fields

Since dc SQUIDs are sensitive to the ambient magnetic field, it is important to be sure that a significant phase shift cannot be produced by a residual magnetic field. We have taken extreme caution to reduce the ambient magnetic field to a low level by nested mu-metal and superconducting shielding. Measurements on Josephson-junction arrays estimate the residual field to be of order 0.1 mG. Because of the flux focusing of the superconducting crystal and films, the field in the SQUID loop can actually be considerably higher, possibly of order 1 mG. For our SQUID areas of typically $30\times30\ \mu\text{m}^2$, this value corresponds to a flux in the loop of order $0.05\Phi_0$,—not negligible, but still less than the spread in the flux shift from trapped flux effects (described below), and far less than the observed $0.5\Phi_0$ shift that signifies d-wave pairing.

5. Trapped flux

A serious concern is the trapping of magnetic flux near the SQUID. A magnetic vortex can couple flux to the SQUID loop and create a shift in the flux modulation pattern that is indistinguishable from the intrinsic phase shift. We account for this by cooling the SQUIDs many times to determine the lowest-energy (most probable) state, which will be the one with no trapped flux. This is the same procedure used to eliminate trapped-flux effects in conventional SQUID detectors. Typically, we find a distribution with a width of order $0.1\Phi_0$ in both edge and corner SQUIDs. This spread does prevent an exact

determination of the phase shift to better than about 5–10%, but is not large enough to blur the distinction between an *s*-wave and *d*-wave pairing symmetry. In addition, we find that the internal consistency and reproducibility of the observed phase shifts essentially rule out the possibility that trapped flux is a significant factor in our results.

6. Corners

It has been pointed out to us that the most obvious difference between our corner SQUIDs and the edge SQUIDs that we use as control samples is the presence of the corner of the crystal inside the SQUID loop. Klemm (1994) in particular has worried that there may be a singularity in the supercurrent flow at the corner, or a difference in the probability of trapping at the corner, compared to the edges, that could give a different response. We find no evidence for either of these effects (Wollman *et al.*, 1994). We have solved for the current flow at the corners and find it to be smooth, even for perfectly sharp corners. Even if singular behavior did occur, it would likely be removed by the rounding of the corner present in any real sample. Flux trapping is also not expected to be different at the corners, since they are substantially rounded on the relevant length scale for pinning (the penetration depth), and the dominant vortex trapping is in the Pb films rather than in the bulk crystals. Consequently, the corner plays no significant role. Also, many measurements on conventional (Nb) SQUIDs, some with corners, exhibit *s*-wave behavior as expected, ruling out corner effects.

C. Experimental details and results

High-quality YBCO single crystals obtained by a flux-melt technique (Rice *et al.*, 1988; Rice and Ginsberg, 1991) are used for the experiment. These crystals have been extensively tested and by any measure used to characterize sample quality (width of the specific-heat peak, normal-state resistivity, linear component of the penetration depth at low temperatures, microwave absorption, . . .) are considered to be among the best available in the world. Typical dimensions are 0.5×0.5 mm^2 in the *a-b* plane, with thicknesses of 20–30 μm. Both twinned and untwinned crystals have been tested and, as noted above, give indistinguishable results. Only crystals with smooth, flat, natural growth faces and a sharp corner are selected; an electron micrograph of the corner of one of the faces is shown in Fig. 6(a). This is crucial, since it ensures that the tunneling is directional and therefore capable of probing the order-parameter asymmetry. Samples are prepared by first thermally evaporating 100–200 nm of Au, masked into sections approximately 50 μm wide, onto the *a-c* and *b-c* faces of the crystals. The gold is then annealed at 400 °C for several hours to produce low-resistance contacts. The crystal is then placed with the *c* axis vertical onto a small droplet of polyamide on a glass slide; the polyamide adheres to the bottom face of the crystal, providing a smooth slope from the substrate up to the bottom of the crystal edges, as illustrated in Fig. 6(b). Finally, a Pb film (800 nm) is deposited through a photoresist mask to make contact with the Au-coated edges, define the SQUID loop, and form electrical leads. A finished sample is shown in Fig. 6(c). The typical SQUID loop size is 30×30^2 μm. Besides the corner SQUID loop connecting junctions on the *a* and *b* faces, several SQUIDs are also fabricated on the edges of each crystal with both junctions on the same face. These edge SQUIDs serve as important control samples: since both junctions sample the same *k*-space direction, they should give an *s*-wave signature independent of the pairing state. The edge SQUIDs can be used to identify any potential problems arising from trapped flux, asymmetries, or other experimental factors.

The YBCO-Au-Pb tunnel junctions formed by this method are SNS (superconductor-normal metal-superconductor) junctions; in some cases, there may also be an insulator barrier between the Au and YBCO, depending on the annealing schedule for the contacts. The critical currents are strongly temperature dependent, increasing sharply as the temperature is lowered. We make the measurements in the temperature range 2–4 K, where I_c is typically 5–500 μA, but we see no evidence that the temperature is a key parameter in these measurements. The junctions exhibit nearly ideal RSJ (resistively shunted junction) current-voltage characteristics, featuring a Josephson supercurrent at zero voltage and a gradual onset of resistance, going asymptotically to a constant level at high current. Figure 7(a) shows the current vs voltage curve for a YBCO-Pb SQUID. Because the modulation is usually small ($<5\%$), it is most easily detected by biasing the SQUID at a constant current and measuring the dynamic resistance vs flux. For all measurements reported here, the SQUIDs are biased in the noise-rounded region below the resistance maximum, as indicated in Fig. 7(b). In this region, an increase in the critical current corresponds to a decrease in the resistance. For most measurements, we use SQUIDs with lower critical currents than the one shown, so that the noise-rounded region is wider, even extending all the way to zero current bias in some cases. The oscillations visible at high bias are due to junction asymmetry as discussed above—the bias current divides unevenly, linking a flux through the SQUID and creating a self-modulation of the SQUID characteristics.

The resistance vs applied flux for a YBCO-Pb SQUID is shown in Fig. 8 for several values of bias current, showing the expected periodic modulation with applied field. Here, the effect of the asymmetric division of the bias current is clearly seen as it creates a current-dependent phase shift in the modulation curves. In order to extract the intrinsic phase shift δ_{ab} inside the YBCO crystal which is of interest to us, it is necessary either to reduce the asymmetry until it is of little significance or to

extrapolate the results to the zero-current limit. We have taken both approaches. Samples that are nearly symmetrical and require little extrapolation, and those in which we could monitor the resistance modulation all the way down to zero bias current, exhibit a minimum resistance at a flux of $(1/2)\Phi_0$. In other samples, it is necessary to extrapolate the phase of the R vs Φ currents to zero bias current by plotting the value of applied flux at which the resistance is a minimum (corresponding to a maximum in the critical current) vs the bias current. This procedure

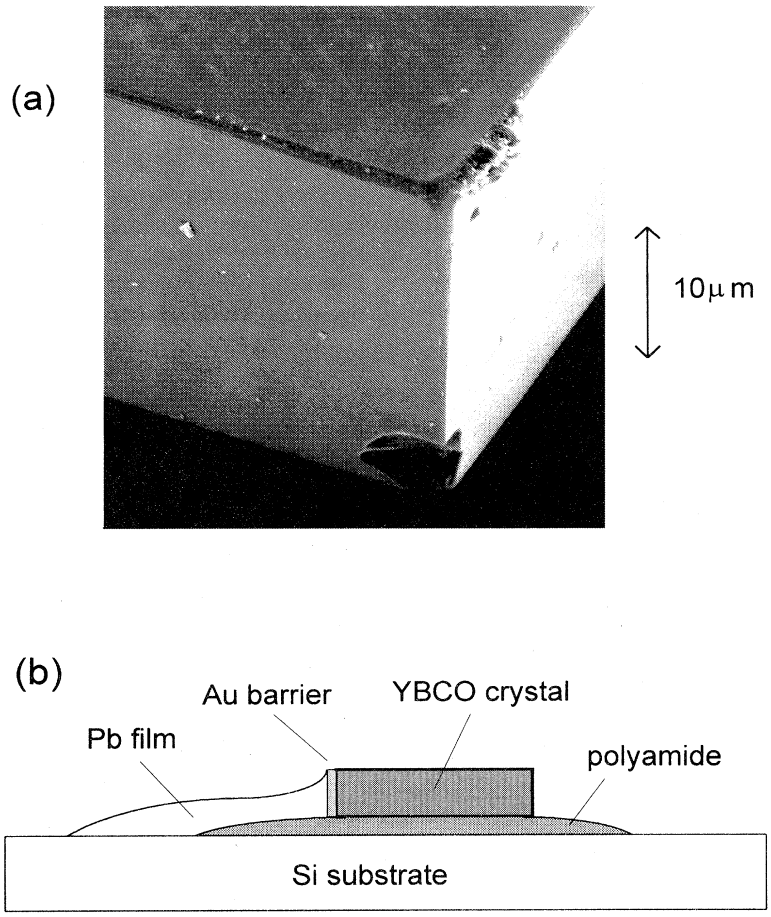

FIG. 6. Sample geometry: (a) Electron micrograph of the corner of a YBCO single crystal used in the experiments, showing the sharpness of the corner and the flatness of the natural growth faces. (b) Schematic of the YBCO-Au-Pb Josephson junctions fabricated on the *a* and *b* edge faces and *ab* corners of the crystal. (c) Electron micrograph of the completed sample, showing the SQUID loop and electrical contacts.

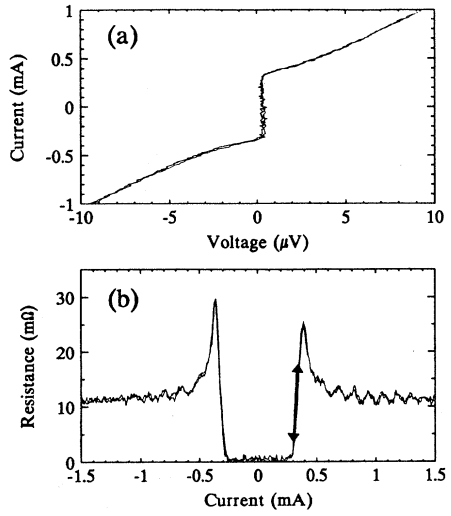

FIG. 7. SQUID electrical characteristics: (a) Current-voltage curves for a YBCO-Au-Pb dc SQUID. Most measurements were made in devices with lower critical currents that exhibit more noise-rounded characteristics. (b) Dynamic resistance vs voltage for the same SQUID. Higher sensitivity is obtained by biasing the SQUID with a constant current in the region indicated and measuring the resistance modulation. From Wollman *et al.*, 1993.

is valid only in the noise-rounded regime near the critical current. It is verified by the experimental data, which do in fact exhibit quasilinear behavior in this regime, and also by the results of the edge SQUIDs, which always extrapolate to zero flux as required independent of the pairing state. For a corner SQUID, *s*-wave pairing gives a zero-current intercept at $\Phi=0$; the $d_{x^2-y^2}$ state would yield an intercept at $\Phi=\Phi_0/2$. In Fig. 9(a), we show measurements and linear extrapolations for seven corner SQUIDs, each cooled slowly in zero field. The slopes, a

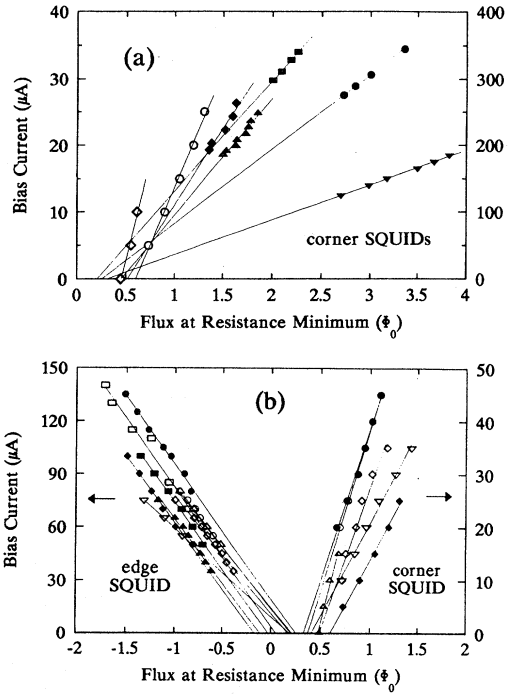

FIG. 9. Measurements of the relative phase in bimetallic SQUIDs: (a) Minima in the SQUID modulation curves extrapolated to zero bias current for seven different samples with varying amounts of asymmetry. An intercept of zero would occur for *s*-wave pairing; the observed intercept of order $\Phi_0/2$ is indicative of the $d_{x^2-y^2}$ symmetry. The distribution is due to magnetic vortices trapped near the SQUID. (b) Comparison of a corner SQUID and edge SQUID on the same crystal cooled down multiple times. As required independent of the pairing state, the edge SQUID extrapolates to zero, but the corner SQUID shows clear evidence for a sign change in the order parameter between orthogonal directions in the crystal. From Wollman *et al.*, 1993.

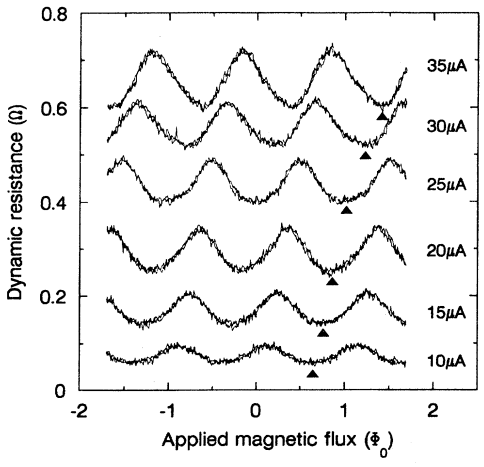

FIG. 8. Modulation of the dynamic resistance vs applied field, showing the expected periodicity and a bias current-dependent phase shift arising from SQUID asymmetries. From Wollman *et al.*, 1993.

measure of the asymmetry, vary over a wide range. The intercepts are distributed in a range centered at $0.5\Phi_0$ with a spread of about $\pm 0.1\Phi_0$. Thus, although the pure *d*-wave signature is not strictly indicated by each sample, each one plotted here—and every other corner SQUID we have studied—does exhibit a significant phase shift of order π consistent with the $d_{x^2-y^2}$ state.

The origin of the distribution of the observed intercepts is trapped magnetic flux. Vortices pinned in the vicinity of the SQUID loop will contribute a flux term that shifts the measured modulation pattern. It is also possible for a vortex to pin near one of the junctions and link flux into the barrier, reducing its critical current and thereby modifying the SQUID asymmetry and hence the slope. We suspect that the dominant pinning sites are at the edges of the Pb thin film; these would generate a flux comparable to that observed in our geometry. To test this, we measured the SQUID modulations of corner samples cooled repeatedly in zero magnetic field. As a

control, we also measured the modulation of edge SQUIDs in which both junctions were on the same face. The results from one pair of SQUIDs on the same crystal are shown in Fig. 9(b). We found a distribution of intercepts clustered around zero phase shift for the edge SQUID, as expected independent of the pairing-state symmetry. However, the corner SQUID intercepts were shifted by $\Phi_0/2$. This gives strong evidence for a sign change in the order parameter in orthogonal directions.

D. Summary of SQUID results

The phase shift we observe in the corner SQUID measurements is strong direct evidence for pairing in a *d*-wave channel. We have observed the π-phase shift, indicative of a sign change in the order parameter between orthogonal directions, in many different corner SQUID samples with a wide range of parameters. The clear and distinct contrast in the behavior of the corner SQUIDs compared to those on the edge of the crystal eliminates most possible spurious effects and points to a strong intrinsic phase anisotropy in the superconducting order parameter of YBCO. As we shall review later, this result has now been confirmed by a number of variations of the SQUID experiment that utilize phase coherence in different configurations.

VI. SINGLE-JUNCTION MODULATION EXPERIMENTS

In the process of carrying out the SQUID measurements, we observed a variation of the SQUID critical current at higher magnetic fields superimposed on the periodic low-field SQUID modulation. This variation arises from the well-known modulation of the individual Josephson-junction critical currents by applied magnetic field threading the barrier region of the junction, an effect analogous to single-slit interference phenomena in optics. This effect suggests an alternative method for determining the pairing-state symmetry, namely, measuring the magnetic-field modulation of the critical current of single YBCO-Pb Josephson junctions. This approach is significant because it avoids many of the potential problems discussed above regarding interpretation of the SQUID experiments and ultimately gives what we believe to be the most striking and convincing demonstration of the sign change in the order parameter inherent in YBCO crystals.

A. Concepts

The effects of an applied magnetic field on the critical current of Josephson tunnel junctions have been extensively studied. The magnetic field penetrating through the barrier region transverse to the tunneling direction forces a gradient in the phase of the order parameter across the width of the junction, resulting in a variation of the local current density and a reduction in the total critical current. In general, calculation of the critical current is complicated by the contribution to the magnetic field in the junction created by the tunneling current itself. However, for junctions that are small compared to the characteristic length scale for self-field effects, the fields from the tunneling currents are negligible. In this "short"-junction regime, the magnetic-field modulation is easily calculated and exhibits a pronounced dependence on the pairing-state symmetry. For a rectangular junction of tunneling area A, width w, magnetic barrier thickness t, and uniform critical current density J_0, the critical current has the usual Fraunhofer diffraction form

$$I_c(\Phi)=J_0 A\left|\frac{\sin(\pi\Phi/\Phi_0)}{(\pi\Phi/\Phi_0)}\right|, \tag{10}$$

which is familiar from single-slit optical diffraction. Here, $\Phi=Bwt$ is the total magnetic flux through the junction for applied magnetic field B. The geometry and expected flux modulation are shown in Fig. 10(a).

To test the symmetry of the pairing state of the YBCO crystal, we measure the critical current of a junction fabricated on the corner of the crystal, as shown in Fig. 10(b). In this geometry, part of the tunneling is into the *a-c* face of the crystal and part is into the *b-c* face. A magnetic field applied along the *c* axis penetrates through each segment of the junction barrier. For an *s*-wave material with either an isotropic or an anisotropic order-parameter magnitude, each face would see the same

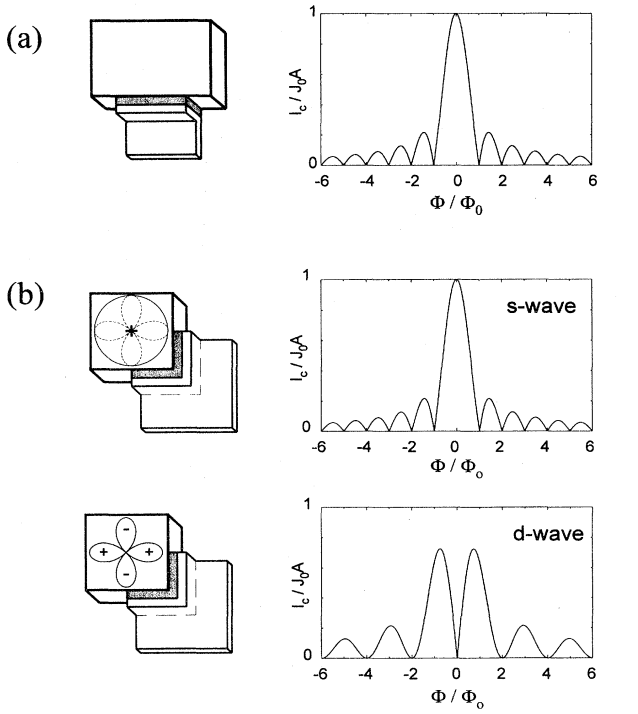

FIG. 10. Scheme for determining the symmetry from single junctions: (a) Fraunhofer diffraction pattern for the critical current modulation of a single Josephson junction with applied magnetic field, analogous to single-slit optical interference. (b) Calculated modulation for a junction straddling the corner for *s*-wave and *d*-wave symmetry.

phase, and the critical current would have the usual Fraunhofer diffraction pattern. However, for a *d*-wave superconductor, the order parameters in the *a* and *b* directions would be of opposite sign, modifying the single-junction diffraction pattern. In a symmetric corner junction (equal junction geometries on the *a* and *b* faces) and uniform critical current density, the critical current modulates according to

$$I_c(\Phi)=J_0 A\left|\frac{\sin^2(\pi\Phi/2\Phi_0)}{(\pi\Phi/2\Phi_0)}\right| . \tag{11}$$

At zero applied field, the current through the two orthogonal faces cancels exactly and the critical current vanishes. Applying a field in either direction increases the critical current, with a maximum value at $\Phi/\Phi_0=0.74$ of about 72% of the maximum current for an *s*-wave junction. The critical current again vanishes when an integer number of flux quanta threads each half of the junction separately, giving a flux modulation period twice that for the edge-junction Fraunhofer diffraction pattern. The critical current modulation vs applied flux for the *s*-wave and *d*-wave cases is shown in Fig. 10(b)—the key feature is whether there is a dip or a peak in the critical current at zero field, which gives a clear and dramatic indication of the pairing-state symmetry.

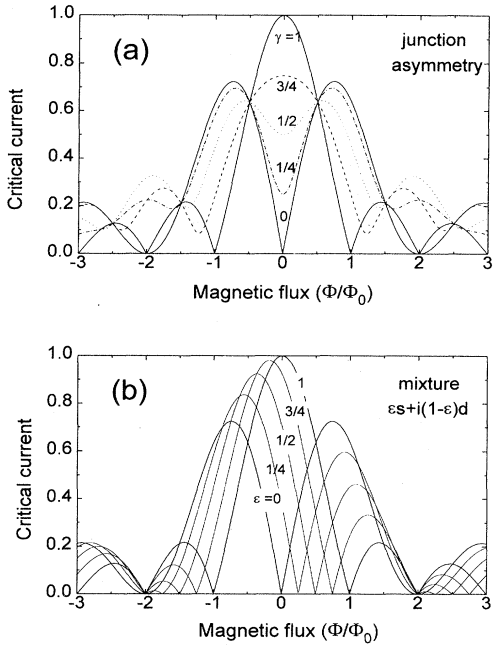

FIG. 11. Modified diffraction patterns for asymmetric junctions and mixed symmetry states: (a) Effect of geometric asymmetry on the single-junction modulation of a corner junction for *d*-wave symmetry, showing the residual critical current at zero field. There would be no effect for *s*-wave symmetry. (b) Single-junction modulation patterns calculated for the $s+id$ state with a fraction ε of *s*-wave component, showing shift in the dip position from zero field and the imbalancing of the peaks as ε increases.

B. Advantages compared to SQUID measurements

Although the SQUID interferometer experiment described above remains the most straightforward and elegant scheme for determining the relative phase, it is clear there are a number of issues that can complicate the interpretation of the data. The single-junction modulation experiments are largely impervious to many of these factors and hence offer significant practical advantages over the SQUID measurements. Before presenting the results of the single-junction measurements, we first consider some of the same factors that we were concerned with in the SQUID measurements, to illustrate why they do not affect the results of the single-junction measurements significantly.

1. Geometry

One advantage is a seemingly trivial one: the single-junction measurements require fabrication of only a single Josephson junction on the crystal instead of the two required for SQUIDs. This, in fact, is a significant experimental benefit because of the limited size of the cuprate crystals and the difficulty in obtaining crystals with extended flat faces. Single-junction measurements can be carried out on crystals on which SQUID fabrication would be impossible. Further, it is easy to obtain crystals with no twin boundaries near the corner, so that measurements can be made on untwinned regions of the sample.

2. Single-junction asymmetry

In the short-junction regime to which we confine our measurements, the only effect of asymmetry is to unbalance the critical currents of the parts of the junctions on the *a* and *b* faces of the crystal. This can occur either as a result of a difference in the widths of the segments or because the critical current densities on the two faces are not the same. Different critical currents do not create a phase shift as in the SQUID measurements, but do prevent the critical current at zero field from canceling exactly, causing the dip to be shallower. As an example, we consider a junction with uniform current density and equal barrier thickness, but with different widths w_a and w_b of the junction segments on the two faces. The critical current for a *d*-wave crystal then depends on the relative asymmetry parameter $\gamma=(w_a-w_b)/(w_a+w_b)$ according to

$$I_c(\Phi,\gamma)=J_0 A\left|\frac{\sqrt{\sin^2(\gamma\pi\Phi/\Phi_0)+[\cos(\pi\Phi/\Phi_0)-\cos(\gamma\pi\Phi/\Phi_0)]^2}}{\pi(\Phi/\Phi_0)}\right|. \tag{12}$$

In particular, the residual critical current at zero field is just $\gamma J_0 A$, a fraction γ of the peak current expected for a uniform s-wave junction. Although I_c is increased at zero field by asymmetry, the mirror symmetry with respect to the applied field is maintained. In Fig. 11, we show calculated diffraction curves for several values of γ; the value $\gamma=0$ is a perfectly symmetric corner junction, while $\gamma=1$ corresponds to a junction fully on one edge.

3. Mixture of *s*-wave and *d*-wave states

It is important to note that the finite critical current in the dip at zero flux cannot be explained by a mixture of s-wave and d-wave states. In fact, analysis of the diffraction patterns of a corner junction for an $s+id$ state reveals that this experiment is an extremely sensitive probe for an s-wave component. The critical current modulation of a symmetric corner junction for an $s+id$ state, as described in Eq. (4), with a fraction ε of s-wave pairing, is given by

$$I_c(\Phi,\varepsilon)=J_0 A\left|\frac{\sqrt{[1-\cos(\pi\Phi/\Phi_0)][1-\cos(\pi\Phi/\Phi_0-\pi\varepsilon)]}}{\pi\Phi/\Phi_0}\right|. \tag{13}$$

This expression reduces easily to the symmetric d-wave pattern for $\varepsilon=0$ and to the usual s-wave Fraunhofer diffraction pattern for $\varepsilon=1$. These curves for those limits and for some intermediate values of ε are plotted in Fig. 11(b). There are two key points. First, the critical current dip for d-wave pairing is not suppressed by an s-wave component. Instead, its flux position shifts linearly by $\varepsilon\Phi_0$. Second, the imbalance in the peak heights for ε small is also approximately proportional to ε, with the fractional imbalance in fact being roughly equal to ε. Thus the measured imbalance is a strong experimental indicator of the s-wave component allowed in an $s+id$ pairing state. An analytical expression for diffraction patterns incorporating simultaneously $s+id$ pairing and junction asymmetry has been given by Miller *et al.* (1995).

4. Residual and trapped magnetic fields

The single-junction coupling area is substantially smaller, typically by a factor of 100, than the dc SQUID loops. As a result, the magnetic-field scale for coupling a flux quantum to the junction is much larger, rendering residual fields relatively unimportant and reducing the probability of flux trapping near the junction. Even more significant, the shape of the diffraction pattern indicates where the zero for magnetic flux in the single junction occurs. For both the s-wave and the d-wave cases, the diffraction pattern is symmetric around zero field in the absence of trapped magnetic flux near the junction. The effect of trapped flux is to skew the diffraction pattern significantly, destroying the mirror symmetry about zero flux. To illustrate the effects of flux trapping, we have calculated the modulation of the critical current with field for junctions with a magnetic vortex trapped near the junction. We model the vortex by assuming a nonuniform magnetic field through the junction barrier, consisting of the uniform applied field plus a Gaussian-distributed flux contribution from the localized vortex near the junction. For both the s-wave and d-wave cases, the diffraction pattern is significantly distorted for all vortex positions, giving a clear signature when a trapped vortex is present. In Fig. 12, we show the critical current modulation for corner junctions on s-wave and d-wave superconductors with a vortex of width 10% of the junction width and total integrated flux $\Phi_0/2$ (the value that has the largest effect) located at several different places along the junction. The key point is that, for the single-junction measurements, symmetry in the diffraction pattern is a strong indication that there is no flux trapping in the junction. This is in sharp contrast to the SQUID measurements, in which trapped flux only shifts the periodic flux modulation and is virtually indistinguishable from an intrinsic phase shift. These considerations indicate that the single-junction modulation patterns of single corner junctions should be a clear indicator of the symmetry of the pairing state in superconductors.

C. Experimental details and results

To test this, we measured the single-junction modulation characteristics of Josephson junctions fabricated on the edges and corners of YBCO single crystals. A typical sample is shown in Fig. 13. The junctions are similar to those used for the SQUID experiments. Typical dimensions are 100 μm wide$\times$20 μm (the crystal thickness), with critical currents at 2.0 K of 20–100 μA and resistances of 100–500 mΩ. For these critical current densities (1–5 A/cm^2), the Josephson penetration depth is much greater than 100 μm, so the junction may be considered to be in the small-junction limit. We determine the critical current by ramping up the bias current until a resistance appears. For very low critical currents (<5

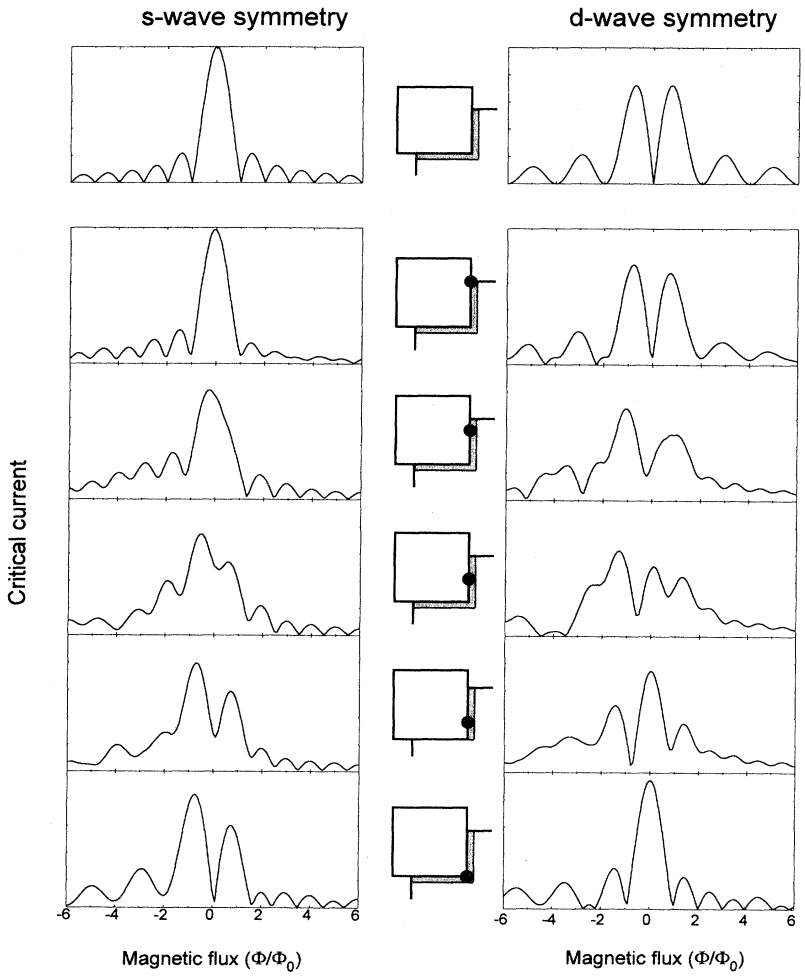

FIG. 12. Effect of trapped magnetic vortices on the single-junction modulation patterns for corner junctions with *s*-wave and *d*-wave symmetry for different vortex locations. Note that the presence of a vortex always breaks the polarity symmetry of the diffraction pattern, providing a clear test for the presence of trapped flux.

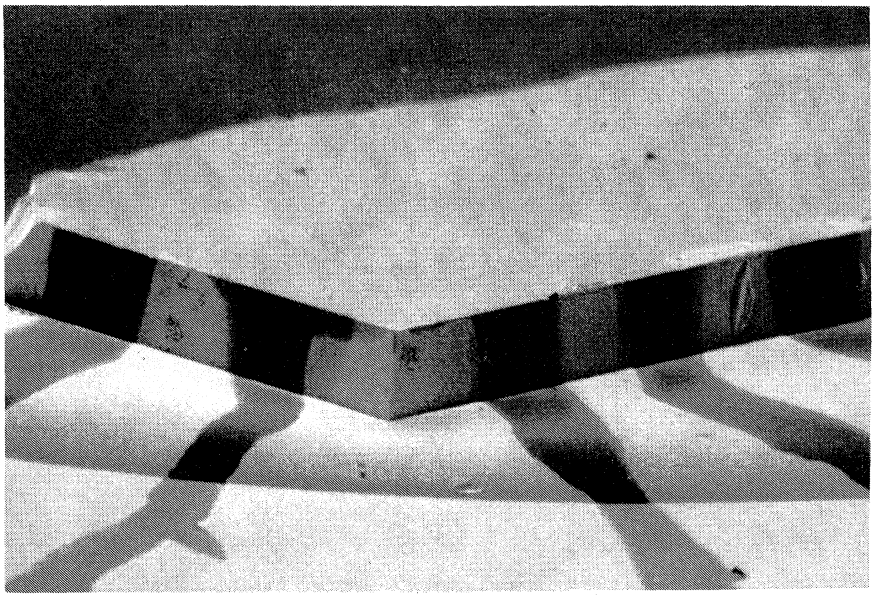

FIG. 13. Electron micrograph of a single-junction sample showing a junction straddling the corner of the crystal and additional junctions on the crystal edges.

μA), it is necessary instead to measure the flux-induced modulation of the dynamic resistance and deduce a value for the critical current. A magnetic field oriented perpendicular to the *a-b* plane of the crystal is applied with a Helmholtz coil. Typically, the magnetic coupling area is about 2×10^{-7} cm^2, so that a local magnetic field of order 1 G is required to put a single flux quantum of magnetic flux through the junction. The applied field required is somewhat lower due to flux focusing by the superconducting crystal and films. External magnetic fields are shielded to less than 1 mG with a room-temperature mu-metal shield and a superconducting Pb foil can. Measurements are made in the temperature range 1.5–4.2 K.

The magnetic-field modulation of single junctions on the edge face and corner of a YBCO crystal are compared in Fig. 14. The critical current of the edge junction exhibits a Fraunhofer-like diffraction pattern with a maximum at zero applied field, as we expect independent of the pairing symmetry. In contrast, the corner-junction modulation on the same crystal is strikingly different, exhibiting a pronounced dip near zero applied field, as expected for the *d*-wave case. The flux periodicity of the corner junction is also different, with all peaks being roughly the same width, whereas the edge junction shows a central peak with a width approximately twice that of the sidelobes, as expected for the Fraunhofer pattern. We have consistently observed this behavior in approximately ten junctions of each type. Because of uncertainties in the effective junction area and the flux-focusing effects, we are not able to determine to actual amount of magnetic flux threading the tunnel junctions. As a result, we cannot determine if the separation of minima in the corner junctions is twice that in the edge devices, as predicted for *d*-wave pairing. As discussed above, we believe that the dip at zero field does not reach zero due to junction asymmetry. An example of a corner junction in which the dip is nearly zero is shown in Fig. 15; in this junction the critical current falls to less than 25% of its peak value and to only about 15% of what we estimate the critical current would be for an *s*-wave junction. We also show the current-voltage characteristic for two values of magnetic flux, showing directly the increase in I_c as the field is increased. The flux modulation patterns are plotted for both polarities of bias current in order to demonstrate the symmetry of the curves. The detailed shape of the diffraction pattern is largely governed by the asymmetry of the corner junction—the dashed curve is the critical current calculated from Eq. (12) for a junction asymmetry $\gamma=0.15$, which fits the observed dip in the critical current at zero field. Note that the shape of the side lobes is also reasonably modeled; in particular, the suppression of the first and fourth side lobes is reproduced.

As discussed above, the symmetry of these two peaks in the corner samples is a strong indication that the pairing state is nearly pure $d_{x^2-y^2}$, with little component of *s*-

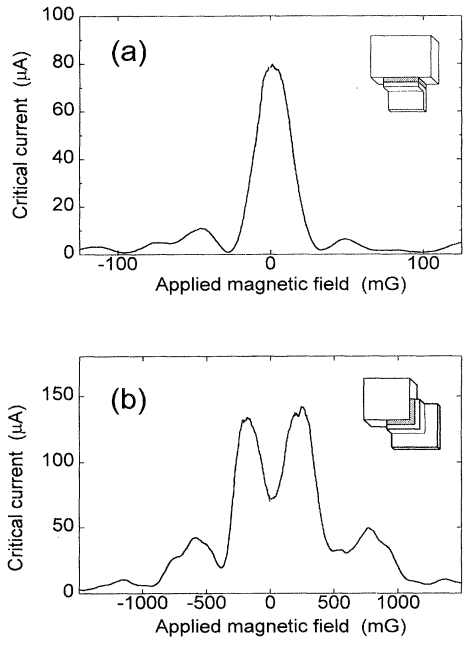

FIG. 14. Modulation patterns measured on (a) an edge junction and (b) a corner junction. The dip at zero field in the corner device is strong evidence for *d*-wave pairing. From Wollman *et al.*, 1995.

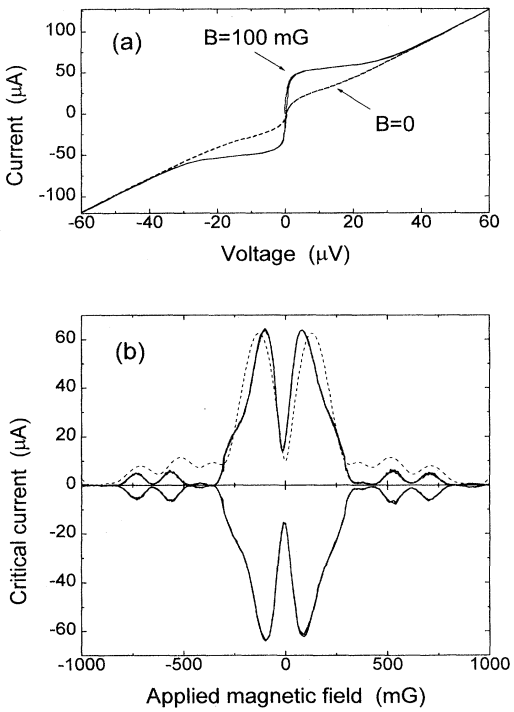

FIG. 15. Measurements on a nearly symmetric single junction on the *a-b* corner of a YBCO crystal: (a) Current-voltage curves for the corner junction showing the increase of the critical current as field is applied in either direction. (b) Corresponding critical current modulation, showing a precipitous dip at zero field and symmetry with respect to both current and field directions. The dashed curve is calculated from Eq. (12) for a junction asymmetry of 15%. From Wollman *et al.*, 1995.

wave possible. For the corner junction in Fig. 15, the peak heights differ by less than 2%, suggesting that the *s*-wave component is no more than this fraction. Based on all of our corner-junction data, we would conservatively put a bound of about 5% on the maximum fractional component of *s* wave consistent with our single-junction modulation experiments.

Finally, we emphasize that the symmetrical dip observed in the critical current is not easily explained nor mimicked by any other mechanism. As far as we know, the observed dip behavior has rarely if ever been reported in the extensive literature on diffraction patterns in single Josephson junctions. This is a key point, since tunneling experiments can sometimes be interpreted in alternate ways because of the sensitivity of the measurements to the complexity of the superconductor surfaces and the tunneling barrier. In this case, however, the key features of the single-junction modulation patterns are very robust because they depend intimately on the interference of the quantum-mechanical phases and average over microscopic details.

D. Summary of single-junction results

The single-junction modulation measurements give what is probably the strongest direct evidence that the superconducting pairing state has the unconventional $d_{x^2-y^2}$ symmetry. The striking difference between the diffraction patterns of the edge and corner junctions, characterized by the sharp dip in the critical current at zero applied field, brings out clearly the anisotropy of the phase of the order parameter without need for calculations or detailed analysis. As we have discussed, the single-junction experiment, though perhaps not as elegant in principal as the basic SQUID interferometer, has many advantages in its ability to eliminate spurious effects. This result has also been generally verified by subsequent single-junction experiments, which have also revealed additional interesting features of Josephson tunneling in cuprate systems. These are reviewed in the next section.

VII. FURTHER PHASE-SENSITIVE TESTS

Since our initial SQUID experiments were published, several other experiments have been reported that are also sensitive to the phase of the order parameter rather than to its magnitude. All of these experiments are based on the same basic principle as the original bimetallic SQUID experiment—the measurement of the relative phase by phase coherence in a multiply connected interferometer geometry. Each experiment gives new insight into the nature of the pairing state and contributes toward the ultimate determination of the pairing symmetry and the mechanism. Most, but not all, confirm the findings of our SQUID and junction experiments that the pairing state of YBCO is *d* wave. In order to assess the present experimental situation, we briefly review these measurements.

A. SQUID experiments

Brawner and Ott of ETH (1994) have reproduced the dc SQUID experiment described above using YBCO-Nb point-contact junctions and a machined Nb cylindrical SQUID body. They detect the critical current modulation with applied flux by applying an ac flux modulation of $(1/2)\Phi_0$ and measuring the ac voltage across the SQUID. The intrinsic phase shift is extracted by looking at the periodic modulation of the ac signal by the bias current, which couples flux to the SQUID as we have discussed. Instead of trying to account for trapped flux and residual fields directly, they compare the results on the bimetallic SQUIDs to those made entirely from Nb. They find a relative phase shift between the two configurations of $160°\pm30°$, in agreement with our results and consistent with *d*-wave symmetry.

Using a scanning SQUID microscope, Tsuei, Kirtley, and co-workers at IBM (Tsuei *et al.*, 1994; Kirtley *et al.*, 1995) have made the first direct measurement of the spontaneous screening currents arising from the π-phase shift between the orthogonal lobes of the order parameter in YBCO. The samples consist of thin-film loops of YBCO deposited onto a tricrystal $SrTiO_3$ substrate. The three regions of the substrate are oriented so that the *c*-axis YBCO films grow with their in-plane *a* and *b* axes rotated successively by 30° in each region; in this geometry, a grain-boundary Josephson junction is formed at each interface. If YBCO is *d* wave, there will be a phase drop of π in each of the three (or in exactly one) section of the film, and a supercurrent must flow (for sufficiently large inductance) to maintain phase coherence as we have discussed; for *s* wave, no spontaneous currents are required. Tsuei *et al.* detect a half odd-integer flux in each ring with three junctions; loops with two or zero junctions always exhibit an integer flux. This beautiful result is strong evidence for a sign change in the order parameter in YBCO and is consistent with *d*-wave pairing symmetry with a maximum limit on the possible *s*-wave component of only 3%. However, because the experiment does not probe orthogonal directions, it is difficult to exclude alternative symmetries, such as the extended *s*-wave pairing state, that also exhibit a sign change.

Spontaneous currents have also been recently detected by scanning SQUID microscopy in bimetallic thin-film dc SQUIDs at the University of Maryland by Wellstood and co-workers (Mathai *et al.*, 1995). YBCO-Nb SQUIDs were fabricated with the junctions on both orthogonal and parallel faces of the oriented YBCO film, corresponding to our corner and edge SQUIDs. A spontaneously generated flux of $(1/2)\Phi_0$ was observed in the corner devices; no net flux was generated in the edge devices. The authors also present a direct method for determining the symmetry and simultaneously testing for

the presence of trapped magnetic flux in the samples by checking for time-reversal symmetry in the current-flux characteristics of the SQUIDs. This eliminates the possibility that the observed results can be accounted for by flux trapping, which is prevalent in the thin-film samples. They find a phase shift of $(0.98\pm0.05)\pi$, in agreement with previous experiments. An interesting conclusion from both the Maryland and IBM thin-film ring experiments is that the observation of the π phase shift implies that the tunneling through the thin-film edge junctions is directional. This was expected for the single-crystal experiments, but is not so obvious in films in which the interface is formed by a grain boundary or by lithography and will be rough on the scale of the coherence length.

The screening currents detected in the IBM and Maryland experiments may have been directly observed previously as the source of the field-cooled paramagnetism in BSCCO composites—the so-called paramagnetic Meissner effect or Wohlleben effect (Braunisch *et al.*, 1992, 1993). It was suggested by Sigrist and Rice (1992) that the spontaneous supercurrents flowing in multiply connected loops between *d*-wave superconducting grains coupled by grain-boundary Josephson junctions could account for this phenomenon. Although the net magnetization for zero-field cooled samples is zero, since the directions of the spontaneous currents are random, field cooling biases the response of the loops, so that they contribute a net paramagnetism. A Josephson-junction model incorporating *d*-wave pairing accounts impressively for both the paramagnetic flux and the anomalous microwave losses reported in these systems. Computer simulations of the effect using a disordered Josephson-junction array model have been carried out by Dominguez *et al.* (1994). A review of this phenomenon appears adjacent to this paper (Sigrist and Rice, 1995).

B. Single-junction experiments

Not all experiments find evidence for *d*-wave symmetry. Chaudari and Lin of IBM (1994) have measured the critical current across a closed grain-boundary junction loop separating regions of a YBCO thin film with *a* and *b* axes misaligned by 45°. For *d* wave, the critical current is expected to be zero by the cancellation of tunneling currents into the positive and negative lobes. Instead the authors observe a finite critical current, and, by isolating different faces of a hexagonal region, find that each face has roughly the same critical current density. This outcome is consistent only with an isotropic *s*-wave order parameter. Millis (1994), however, has proposed that this result may be consistent with *d*-wave symmetry when the phase contributions from the tunneling currents are taken into account. Since the IBM junctions are in the long-junction limit, it is energetically favorable to allow a Josephson vortex to nucleate along the interface (e.g., at a corner). This satisfies the phase coherence constraints while allowing each junction to carry its maximum critical current, mimicking an *s*-wave result.

The long-junction limit has also been discussed by researchers at the University of Houston (Miller *et al.*, 1995) who have measured the critical current diffraction patterns for YBCO single junctions fabricated on tricrystal substrate. The geometry is the single-junction version of the IBM ring experiments. Although the diffraction patterns have complex structure, probably due to junction roughness and inhomogeneities in the critical current density, the authors do observe a pronounced dip in the critical current for low-current-density junctions in the short-junction limit, analogous to that observed in our single YBCO-Pb junction corner measurements. In the long-junction regime, the dip is absent and the critical current peaks at zero magnetic field. Both of these results are consistent with *d*-wave pairing and provide verification that self-field effects can mask intrinsic *d*-wave behavior.

C. *C*-axis tunneling experiments

In addition to the experiments based on phase coherence in the *a*-*b* plane, there are several studies of Josephson tunneling from a conventional superconductor into the *c* axis of a cuprate superconductor. In contrast to the situation in the *a* or *b* directions, it is difficult to observe Josephson supercurrents in junctions fabricated on the *c* axis. Most studies have concluded that the critical current density for *c*-axis (001) oriented films is zero, whereas substantial current densities have been observed in *a*-axis (100) films. Two possible explanations are commonly given for this phenomenon. One point of view is that Josephson tunneling is suppressed by contamination of the cuprate surface, probably due to deoxygenation of the top few CuO planes, a consequence of the extremely short *c*-axis coherence length of the cuprates (<10 Å). An alternate interpretation is that YBCO is a *d*-wave superconductor, creating a cancellation of the supercurrent into the lobes of opposite polarity. This is a subtle argument, since the *d*-wave lobes represent the order parameter in the *a*-*b* plane. The prevailing model is that conduction along the *c* axis occurs via Josephson tunneling between CuO_2 planes and that there is no Fermi surface in that direction. However, although the process by which *c*-axis tunneling current couples into the *a* and *b* planes inside the crystal is not fully understood, it is reasonable to assume that electrons tunneling into the cuprate would sample the order parameter according to the component of their momentum in the *a*-*b* plane. In this case, tunneling into a tetragonal crystal would give a zero supercurrent. The current could be finite, however, in a single crystal with orthorhombic symmetry, since the size of the $+$ and $-$ lobes are likely to be different.

Recently, however, the situation has been complicated by reports from at least two groups of experiments with finite supercurrents into the *c* axis of YBCO. Both the group of Dynes at UC San Diego (Sun *et al.*, 1994) and that of Iguchi at Tsukuba, Japan (Iguchi and Wen, 1994) have observed supercurrents through YBCO-Pb tunnel

junctions on the c-axis faces of YBCO single crystals and films, and measured the modulation of the critical current as a function of magnetic field applied orthogonal to the junction. This result seems to be inconsistent with a $d_{x^2-y^2}$ pairing state, since the supercurrent is expected to cancel out in the oppositely-signed order-parameter lobes. The primary experimental concern is that tunneling into exposed a and b faces may dominate the supercurrent. This is certainly possible, since etches used to prepare the YBCO surface are known to create pits at strong concentrations. In fact, Iguchi *et al.* interpret their data in this manner, attributing the dip they see at zero applied field in the diffraction patterns to a mixture of tunneling into a and b faces and into a-b corners, citing the single-junction results for edges and corners of a d-wave superconductor that we discussed above. This picture supports d wave, but is overly simplified, since it neglects the global phase coherence between all of the tunneling regions. In contrast, Sun *et al.* observe nearly ideal Fraunhofer diffraction patterns in their junctions, suggesting uniform current densities. Further, the modulation period is consistent with the known c-axis penetration depth of YBCO and the full geometric width of the junction. This seems to justify the authors' claim that they are tunneling only into the c-axis face, from which they conclude that there must be a substantial s-wave component to the pairing state in YBCO. This result is inconsistent with the SQUID and junction modulation experiments, to the accuracy that they show a phase change of exactly π, and with magnitude measurements to the extent that they show a fully-formed node. An alternate explanation is that there exists a spontaneous symmetry breaking of the d-wave order parameter, causing one lobe of the d-wave pattern to be dominant. This would naturally arise from the orthorhombicity of YBCO if there were an imbalance in the areal densities of a-axis vs and b-axis oriented planes in the plane, or could perhaps be induced from the tunneling interaction between the YBCO and the conventional superconductor. This remains the most interesting experiment that seems to contradict the d-wave pairing scenario.

VIII. PRESENT STATUS—THE CASE FOR *D*-WAVE PAIRING

Both our SQUID and single-junction modulation experiments give strong evidence for a phase shift of order π in the phase of the order parameter between orthogonal directions in YBCO. These results strongly support a superconducting pairing state with $d_{x^2-y^2}$ symmetry and seem impossible to explain by any purely s-wave state or any mixture state incorporating any substantial s-wave component. Most of the other reported phase coherence experiments employing different materials, geometries, and techniques verify and strengthen this conclusion; a few do not. A compilation of the key experiments and their results is shown in Table I. The stars indicate which pairing symmetries are consistent with the results of the experiment. The question marks indicate that alternate explanations have been suggested that seem to reconcile the results with additional symmetries. In the column for the mixture of s- and d-wave states, the number given is the maximum fraction of s-wave component consistent with the experimental results; for experiments

TABLE I. Summary of experiments designed to determine the symmetry of the superconducting pairing states.

Experiment	Research group	Isotropic s wave	Anisotropic s wave	Pure $d_{x^2-y^2}$	Mixture $s+id$
Magnitude measurements	many		*	*	*
Penetration depth	U. of British Columbia (Hardy, Bonn, ...)		*	*	2%
dc SQUID interferometry	U. of Illinois (Wollman, Van Harlingen, ...)			*	10%
dc SQUID interferometry	ETH (Brawner and Ott)			*	10%
dc SQUID magnetometry	U. of Maryland (Mathai, Wellstood, ...)			*	5%
Tricrystal ring magnetometry	IBM (Tsuei, Kirtley, ...)			*	3%
Biepitaxial junctions	IBM (Chaudari, Lin, ...)	*	?	?	?
Single-junction modulation	U. of Illinois (Wollman, Van Harlingen, ...)			*	5%
Single-junction modulation	U. of Houston (Miller, *et al.*)			*	25%
c-axis diffraction	U. of California, San Diego (Sun, Dynes, ...)	*	*	?	*
c-axis diffraction (a-b steps)	U. of Tsukuba, Japan (Iguchi and Wen)			*	25%

sensitive only to the magnitude of the order parameter, this is also the minimum magnitude of the gap along the node directions.

The evidence for d-wave symmetry in YBCO seems to be solid and growing. Virtually every experiment specifically designed to probe the phase anisotropy finds evidence for the sign change in the order parameter in orthogonal directions. Magnitude probes suggest that the anisotropy is very strong and is consistent with the fully-formed nodes characteristic of $d_{x^2-y^2}$ symmetry. There remain, however, important questions about the c-axis tunneling and other experiments that must be fully resolved before the pairing state is definitively established and accepted.

IX. FUTURE DIRECTIONS

Although the symmetry of the pairing state of YBCO is perhaps not definitively established, the growing experimental evidence for unconventional pairing in YBCO makes it appropriate to consider what directions research in this field will take in the next few years. The immediate focus is likely to be application of the techniques described here to other cuprate materials beyond YBCO. It is important to establish whether the apparent d-wave pairing is specific to YBCO or whether it also occurs in materials with similar CuO layered structure. Although it is highly appealing to believe that a single microscopic model is responsible for the superconductivity in all of the high-temperature superconductors and that they will all exhibit the same pairing symmetry, this needs to be established by experiment. In fact, there are some indications that the situation might not be so simple. For example, the medium-temperature ($T_c = 30$ K) superconductor NdCeCuO has CuO planes much like YBCO, but preliminary measurements of the penetration depth at low temperatures give an exponential behavior, signifying a fully formed s-wave energy gap (Anlage *et al.*, 1994). The highest-temperature ($T_c = 150$ K) cuprate system of all, HgBaCaCuO, also shows evidence for energy gaps in point-contact tunneling, in sharp contrast to YBCO (Chen *et al.*, 1994). Since these materials are not yet available in single crystals or thin films of the quality and purity of the YBCO samples, phase-sensitive measurements of the type discussed here stand as the most promising and definitive approach to probing their pairing symmetry.

Establishing whether the d-wave symmetry indicated in YBCO is a characteristic property of the cuprates or is specific to that system will place strong constraints on the nature of a comprehensive theory of superconductivity for the cuprates. However, although the phase-sensitive measurements are the best way to determine the symmetry of the pairing state, they are not able to identify the microscopic mechanism for the pairing. This will have to be established by impurity-doping experiments, tunneling spectroscopy measurements, and other techniques that are sensitive to the interactions that mediate the superconducting pairing.

Ultimately, it will be interesting to apply the phase-sensitive interferometry tests to other superconducting systems that may also be unconventional. The leading candidates are the heavy-fermion superconductors UPt_3 and UBe_{13}, which are now believed to exhibit a type of d-wave pairing and may, in the case of UPt_3, have two order parameters and break time-reversal symmetry. Experiments are now underway in our laboratory to determine the pairing symmetry of these materials by Josephson tunneling and dc SQUID experiments. It would be fitting ultimately to apply the interferometer configuration to the heavy-fermion materials for which it was originally proposed.

ACKNOWLEDGMENTS

The work described here is a result of important contributions from a number of very talented researchers at the University of Illinois at Urbana-Champaign. Most significant have been the efforts of graduate student David Wollman, whose skill in fabricating the samples and dedication in carrying out extensive measurements have been critical to the success of this project. Another essential element of the experiments has been access to what are likely the world's best single crystals of YBCO, grown and characterized in the group of Donald Ginsberg by his postdoctoral associates Wonchoon Lee and John Giapintzakis. I am sincerely grateful to Tony Leggett, who initially suggested the elegant phase-sensitive SQUID measurement and who has been a constant source of good ideas, theoretical support, and right answers throughout this work. I also acknowledge the inspiration and insight gained through discussions with my superconductivity colleagues at Urbana, especially Nigel Goldenfeld, Miles Klein, Myron Salamon, and Charles Slichter. Finally, the primary motivation for the tests of the pairing symmetry has been the theoretical modeling of David Pines, who has maintained and has now demonstrated that the $d_{x^2-y^2}$ state is a viable candidate for the pairing state of the cuprates.

This work was initially funded by the National Science Foundation through Materials Research Laboratory under Grant No. DMR-89-20538, and is now supported by the Science and Technology Center for Superconductivity under Grant No. DMR91-20000. I also acknowledge extensive use of the facilities and capabilities of the Microfabrication Laboratory of the Materials Research Laboratory at the University of Illinois.

REFERENCES

Anlage, S. W., D.-H. Wu, J. Mao, S. N. Mao, X. X. Xi, T. Venkatesan, J. L. Peng, and R. L. Greene, 1994, Phys. Rev. B **50**, 523.

Annett, J. F., N. Goldenfeld, and S. R. Renn, 1990, in *Physical Properties of High Temperature Superconductors II,* edited by

D. M. Ginsberg (World Scientific, Singapore), p. 571.
Annett, J. F., N. Goldenfeld, and S. R. Renn, 1991, Phys. Rev. B **43**, 2778.
Bardeen, J., L. N. Cooper, and J. R. Schrieffer, 1957, Phys. Rev. **108**, 1175.
Barrett, S. E., J. A. Martindale, D. J. Durand, C. P. Pennington, C. P. Slichter, T. A. Friedmann, J. P. Rice, and D. M. Ginsberg, 1991, Phys. Rev. Lett. **66**, 108.
Bednorz, J. G., and K. A. Muller, 1986, Z. Phys. B **64**, 189.
Bickers, N. E., D. J. Scalapino, and S. R. White, 1989, Phys. Rev. Lett. **62**, 961.
Bonn, D. A., S. Kamel, K. Zhang, R. Liang, D. J. Baar, E. Klein, and W. N. Hardy, 1995, University of British Columbia preprint.
Brandow, B., 1994, in *Strong Correlated Electronic Materials: The Los Alamos Symposium 1993,* edited by K. Bedell (Addison-Wesley, Reading, Mass.), p. 611.
Braunisch, W., N. Knauf, V. Kataev, S. Neuhausen, A. Grütz, A. Kock, B. Roden, D. Khomskii, and D. Wohlleben, 1992, Phys. Rev. Lett. **68**, 1908.
Braunisch, W., N. Knauf, G. Bauer, A. Kock, A. Becker, B. Freitag, A. Grütz, V. Kataev, S. Neuhausen, B. Roden, D. Khomskii, and D. Wohlleben, 1993, Phys. Rev. B **48**, 4030.
Brawner, D. A., and H. R. Ott, 1994, Phys. Rev. B **50**, 6530.
Chakravarty, S., A. Sudbo, P. W. Anderson, and S. Strong, 1993, Science **261**, 337.
Chaudari, P., and S.-Y. Lin, 1994, Phys. Rev. Lett. **72**, 1084.
Chen, J., J. F. Zasadzinski, K. E. Gray, J. L. Wagner, and D. G. Hinks, 1994, Phys. Rev. B **49**, 3683.
Cooper, S. L., and M. V. Klein, 1990, Comments Condens. Mater. Phys. **15**, 99.
Dagotto, E., 1994, Rev. Mod. Phys. **66**, 763.
Devereaux, T. P., D. Einzel, B. Stadlober, R. Hackl, D. H. Leach, and J. J. Neumeier, 1994, Phys. Rev. Lett. **72**, 396.
Domínguez, D., E. A. Jagla, and C. A. Balseiro, 1994, Phys. Rev. Lett. **72**, 2773.
Fong, H. F., B. Keimer, P. W. Anderson, D. Reznik, F. Dogan, and I. A. Aksay, 1995, Princeton University preprint.
Geshkenbein, V. B., and A. I. Larkin, 1986, JETP Lett. **43**, 395.
Geshkenbein, V. B., A. I. Larkin, and A. Barone, 1987, Phys. Rev. B **36**, 235.
Giaver, I., 1960, Phys. Rev. Lett. **5**, 147.
Hardy, W. N., D. A. Bonn, D. C. Morgan, R. Liang, and K. Zhang, 1993, Phys. Rev. Lett. **70**, 3999.
Hirschfeld, P. J., and N. Goldenfeld, 1993, Phys. Rev. B **48**, 4219.
Iguchi, I., and Z. Wen, Phys. 1994, Phys. Rev. B **49**, 12 388.
Josephson, B. D., 1962, Phys. Lett. **1**, 251.
Kane, J., Q. Chen, K.-W. Ng, and H.-J. Tao, 1994, Phys. Rev. Lett. **72**, 128.
Kirtley, J. R., C. C. Tsuei, J. Z. Sun, C. C. Chi, L. S. Yu-Jahnes, A. Gupta, M. Rupp, and M. B. Ketchan, 1995, Nature **373**, 225.
Klemm, R. A., 1994, Phys. Rev. Lett. **73**, 1871.
Kotliar, G., 1988, Phys. Rev. B **37**, 3664.
Laughlin, R. B., 1994, Stanford University preprint.
Leggett, A. J., 1993, private communication.
Li, Q. P., B. E. Koltenbach, and R. Joynt, 1993, Phys. Rev. B **48**, 437.
Martindale, J. A., S. E. Barrett, K. E. O'Hara, C. P. Slichter, W. C. Lee, and D. M. Ginsberg, 1993, Phys. Rev. B **47**, 9155.
Mathai, A., Y. Gim, R. C. Black, A. Amar, and F. C. Wellstood, 1994, University of Maryland preprint.
Miller, J. H., Q. Y. Ying, Z. G. Zou, N. Q. Fan, J. H. Xu, M. F. Davis, and J. C. Wolfe, 1995, Phys. Rev. Lett. **74**, 2347.
Millis, A., 1994, Phys. Rev. B **49**, 15408.
Monthoux, P., A. Balatsky, and D. Pines, 1992, Phys. Rev. B **46**, 14803.
Monthoux, P., and D. Pines, 1993, Phys. Rev. B **47**, 6069.
Monthoux, P., and D. Pines, 1994, Phys. Rev. B **49**, 4261.
Moriya, T., Y. Takahashi, and K. Ueda, 1990, J. Phys. Jpn. **59**, 2905.
Pines, D., 1995, in *High T_c Superconductivity and the C_{60} Family,* edited by T. D. Lee and H. C. Ren (Gordon and Breach, New York).
Rice, J. P., and D. M. Ginsberg, 1991, J. Cryst. Growth **109**, 432.
Rice, J. P., B. G. Pazol, D. M. Ginsberg, T. J. Moran, and M. B. Weissmann, 1988, J. Low Temp. Phys. **72**, 345.
Rokhsar, D. S., 1993, Phys. Rev. Lett. **70**, 493.
Scalapino, D. J., 1995, Phys. Rep., in press.
Shen, Z.-X., D. S. Dessau, B. O. Wells, D. M. King, W. E. Spicer, A. J. Arko, D. Marshall, L. W. Lombardo, A. Kapitulnik, P. Dickinson, S. Doniach, J. diCarlo, A. G. Loeser, and C. H. Park, 1993, Phys. Rev. Lett. **70**, 1553.
Sigrist, M., and T. M. Rice, 1992, J. Phys. Soc. Jpn. **61**, 4283.
Sigrist, M., and T. M. Rice, 1995, Rev. Mod. Phys. **67**, 491 (1994).
Slichter, C. P., 1994, in *Strongly-Correlated Electron Systems,* edited by K. S. Bedell *et al.* (Addison-Wesley, New York), p. 427.
Stupp, S. E., and D. M. Ginsberg, 1991, in *Physical Properties of High Temperature Superconductors III,* edited by D. M. Ginsberg (World Scientific, Singapore), p. 1.
Sun, A. G., D. A. Gajewski, M. B. Maple, and R. C. Dynes, 1994, Phys. Rev. Lett. **72**, 2267.
Tsuei, C. C., J. R. Kirtley, C. C. Chi, L. S. Yu-Jahnes, A. Gupta, T. Shaw, J. Z. Sun, and M. B. Ketchen, 1994, Phys. Rev. Lett. **73**, 593.
Ueda, K., T. Moriya, and Y. Takahashi, 1992, J. Phys. Chem. Solids **53**, 1515.
Wollman, D. A., D. J. Van Harlingen, W. C. Lee, D. M. Ginsberg, and A. J. Leggett, 1993, Phys. Rev. Lett. **71**, 2134.
Wollman, D. A., D. J. Van Harlingen, J. Giapintzakis, and D. M. Ginsberg, 1995, Phys. Rev. Lett. **74**, 797.
Wollman, D. A., D. J. Van Harlingen, W. C. Lee, D. M. Ginsberg, and A. J. Leggett, 1994, Phys. Rev. Lett. **73**, 1872.
Yu, R. C., M. B. Salamon, and W. C. Lee, 1992, Phys. Rev. Lett. **69**, 1431.
Yu, F., M. B. Salamon, A. J. Leggett, W. C. Lee, and D. M. Ginsberg, 1995, University of Illinois preprint.

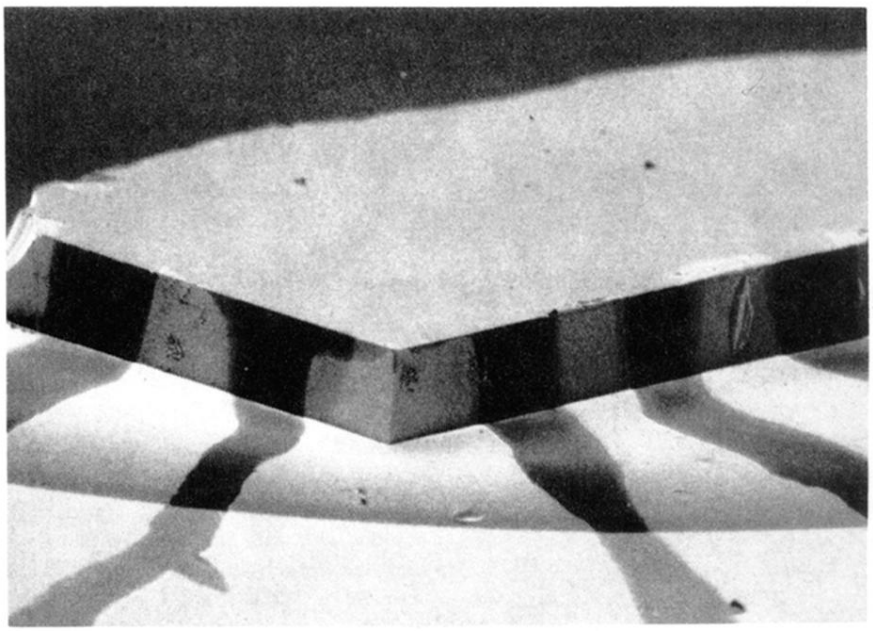

FIG. 13. Electron micrograph of a single-junction sample showing a junction straddling the corner of the crystal and additional junctions on the crystal edges.

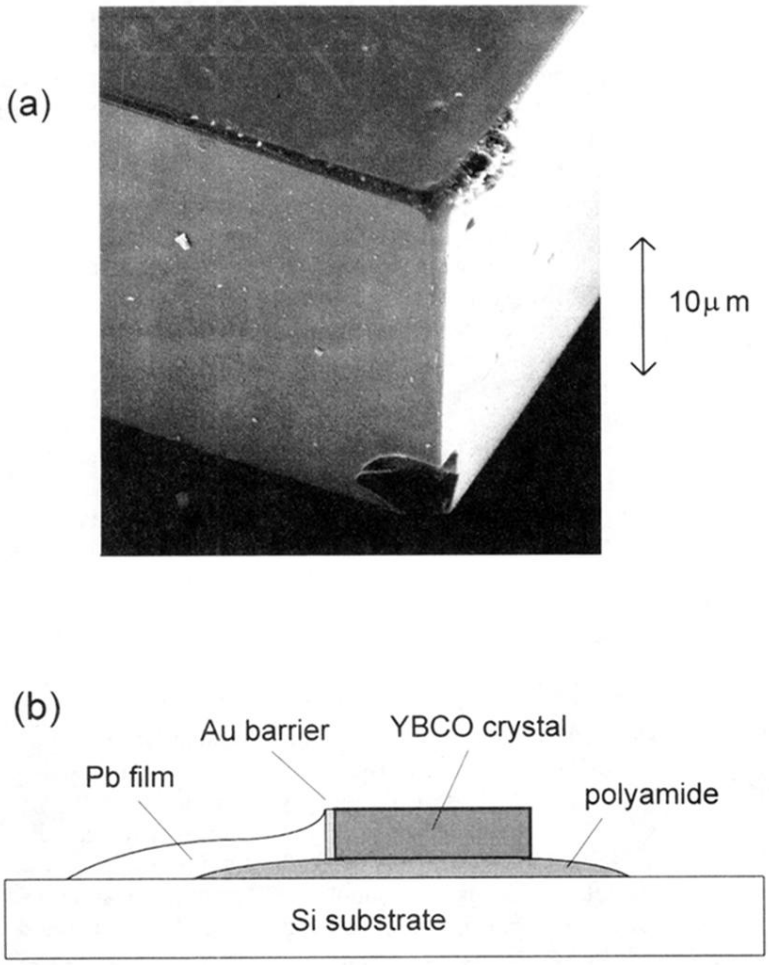

FIG. 6. Sample geometry: (a) Electron micrograph of the corner of a YBCO single crystal used in the experiments, showing the sharpness of the corner and the flatness of the natural growth faces. (b) Schematic of the YBCO-Au-Pb Josephson junctions fabricated on the *a* and *b* edge faces and *ab* corners of the crystal. (c) Electron micrograph of the completed sample, showing the SQUID loop and electrical contacts.